



## Research paper

# Determination of force in single cable plane prestressed concrete polygonal line tower cable-stayed bridge based on minimum bending energy

Y. Li<sup>1</sup>, T. Guo<sup>2</sup>, L. Bao<sup>3</sup>, F. Wang<sup>4</sup>

**Abstract:** The cable force of a cable-stayed bridge plays a vital role in its internal force state. Different cable forces on both sides of the main tower make the force characteristics of the polygonal-line tower quite different from those of the straight-line tower. Therefore, the determination of the cable force of the polygonal-line tower cable-stayed bridge is a crucial aspect of any evaluation of its mechanical characteristics. A single-cable plane prestressed concrete broken-line tower cable-stayed bridge is taken as a case study to conduct a model test and theoretical cable force determination. The reasonable cable force of the bridge is determined by the minimum bending energy method combined with false load and internal force balance methods. analysis includes a comparison between cable force calculation results, model test results, and the design value of the actual bridge. The distribution law of the dead load cable force of the completed bridge is determined accordingly.

**Keywords:** cable-stayed bridge, polygonal tower, finite element method, minimum bending energy method

<sup>1</sup> Prof., PhD., School of Transportation Engineering, Shenyang Jianzhu University, Shenyang 110168, China, e-mail: [lyfneu@126.com](mailto:lyfneu@126.com)

<sup>2</sup> Master., School of Transportation Engineering, Shenyang Jianzhu University, Shenyang 110168, China, e-mail: [ArronGG@126.com](mailto:ArronGG@126.com), ORCID: <https://orcid.org/0000-0003-4945-5770>

<sup>3</sup> Prof., PhD., School of Transportation Engineering, Shenyang Jianzhu University, Shenyang 110168, China, e-mail: [13516094255@163.com](mailto:13516094255@163.com), ORCID: <https://orcid.org/0000-0001-5582-1103>

<sup>4</sup> Prof., PhD., School of Transportation Engineering, Shenyang Jianzhu University, Shenyang 110168, China, e-mail: [wangfuchun1967@163.com](mailto:wangfuchun1967@163.com)

## 1. Introduction

The cable force of a cable-stayed bridge can be adjusted between the construction stage and completion stage. There is a state in each cable-stayed bridge that can be used to optimize the mechanical performance of the whole structure, so there is also a set of cable forces that ensure a certain target reflecting the optimal mechanical performance [1-3] under a deterministic load satisfying the relevant structural requirements. This set of cable forces can be considered the optimal cable force under the bridge's reasonable internal force.

Domestic and foreign scholars have determined cable force in cable-stayed bridges via theoretical analyses, field tests, and indoor model tests [3–7]. Tao et al [8] studied the optimization of cable force in a prestressed concrete cable-stayed bridge design; the minimum bending strain energy of the tower beam was considered to be the optimization goal and the structural stress and cable force were constraint conditions. Zhou et al [9] optimized cable force in a cable-stayed bridge with a thin-cable steel box girder, with the minimum bridge alignment as the objective function and structural stress and deformation as constraints. The Baldomir et al [10] analyzed the optimal cable force based on the minimum amount of cable used in the cable-stayed bridge as the optimization objective; the cable force, main beam, and bridge tower deformation were considered the constraints. Martins et al [11] established a cable force optimization model that includes the cable force, main girder and bridge tower deformation, and main girder and bridge tower stress constraints.

The dense cable system cable-stayed bridge has many cables, each with a different design value. Hassan et al. [12] and Wu et al. [13] used a genetic algorithm to determine the optimal cable force of a long-span cable-stayed bridge. Sung et al [14] attempted to optimize cable force in a long-span cable-stayed bridges via particle swarm optimization algorithm. These methods provide reasonable cable force optimization results, however, they are tailored to straight-tower bridge designs. The force characteristics of the polygonal-line tower markedly differ from straight-tower designs, as there are different cable forces on either side of the main tower. Accurate determination of the cable force in the polygonal-line tower cable-stayed bridge is key to comprehensively and effectively understanding its mechanical characteristics.

The static balance characteristics of a real-world, prestressed concrete polygonal-line tower cable-stayed bridge were utilized in this study to establish a theoretical formula of its arrangement and local balance. The minimum bending energy method, false load method, and internal force balance

method were used to determine the reasonable bridge cable force. The calculation results, model test results, and design values of the actual bridge were compared to determine the distribution law of the dead-load cable force of the bridge.

## 2. Research background

The Fumin Bridge in Shenyang, China was taken as a case study. Its primary structure is a single cable plane PC cable-stayed bridge 420 m in length with an 89 m side span and 242 m middle span. The central tower is a box-shaped section. The main structure is 67.5 m in height with a 33.9 m bend angle of the central tower above the bridge deck. The angle between the lower tower body and the horizontal plane is 75 degrees and the angle between the upper tower body and lower tower body is 7.5 degrees. The bridge contains a total of 200 galvanized high-strength steel wires with specifications of 301 –  $\phi 7$ , 241 –  $\phi 7$ , 211 –  $\phi 7$ , and 151 –  $\phi 7$ , as shown in Figure 1.

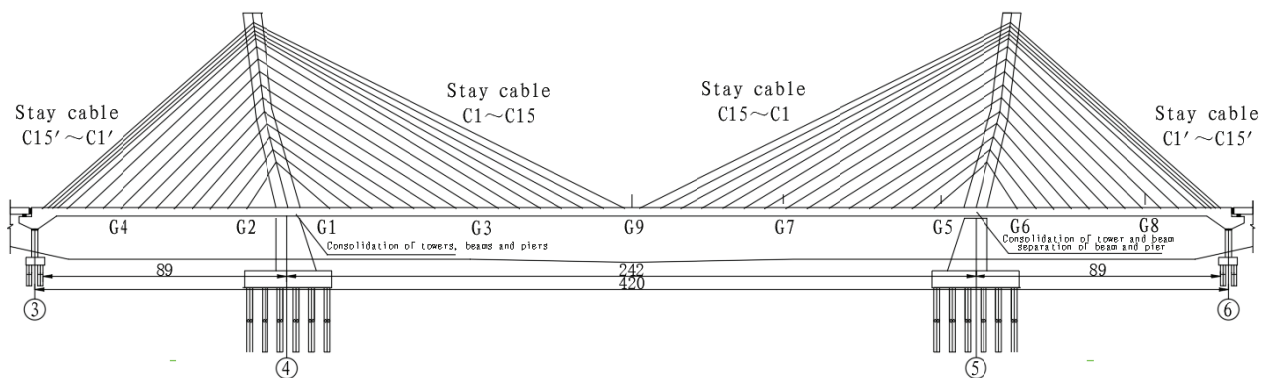


Fig. 1. Arrangement of main bridge (unit: m)

## 3. Model design and production

### 3.1. Design model

A structural model was constructed based on three similarity theorems to obtain results as close as possible to the objective reality [15–19]. According to the characteristics of the Fumin Bridge, the optimal geometric scaling ratio for the model was determined to be 1:40. The section stiffness of the Fumin Bridge test model is similar to that of the bridge prototype. The test model is geometrically similar to the bridge prototype and was established in accordance with the largest possible scale. The load of the test model was proportionally reduced according to the actual load

ratio. Additionally, the materials of the bridge testing model and prototype are similar and the test model has the same boundary conditions as the real bridge.

Model testing of a cable-stayed bridge requires certain site conditions, loading conditions, and test-related costs. Selecting the optimal geometric scale is the primary problem to be solved in the model design process. Large-scale models are easy to produce and experimental data are easy to collect, but are costly, labor-intensive, and require large test sites and certain loading equipment. A small-scale model requires only a lightweight load, but it is relatively difficult to build or equip with test instruments; additionally, the measurement error is relatively large. It is necessary to weigh various test conditions and requirements before selecting the most appropriate scale for model-making. The layout of the full-bridge model used in this study is shown in Figure 2.

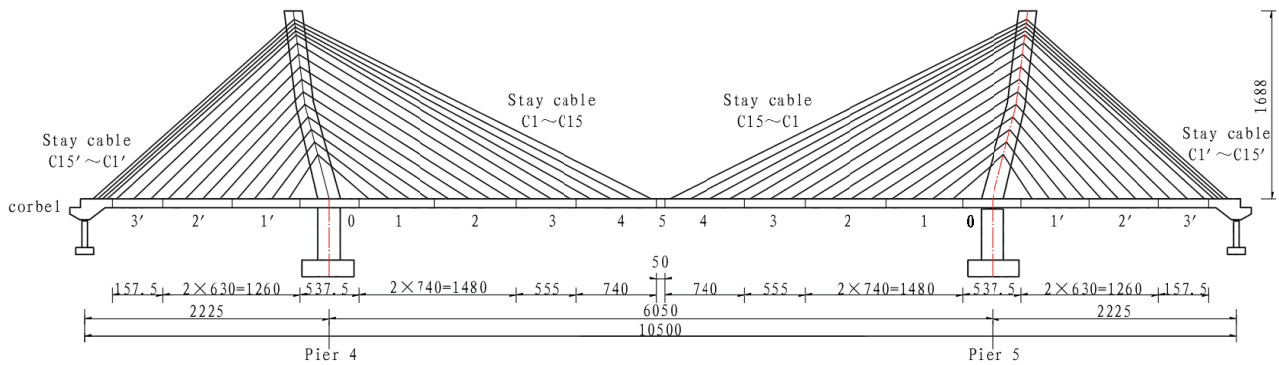


Fig. 2. General arrangement of model (unit: mm)

### (1) Stay cable design.

The stay cable of the model is made of high-strength steel wire with an elastic modulus ratio equal to 1. The cross-sectional area of the stay cable in the model is expressed as follows:

$$(3.1) \quad A_m = A_p (1/40^2)$$

where  $A_m$  is the model area and  $A_p$  is the real bridge area.

The model stay cable has 14–32 high-strength steel wires 0.5 mm in diameter. The end of the stay cable is connected to the bridge tower and box girder via thread, which allows it to be easily adjusted. A vibrating wire type load cell at the joint measures the cable force of the stay cable. To accurately reflect the mechanical characteristics of structural nonlinearity, load compensation was performed for the dead weight of the cable and an additional mass method was adopted.

(2) Main tower design.

The external contour dimensions of the main tower section remain basically unchanged, so there is a similar relationship between the moment of inertia and the cross-sectional area. The main tower of the bridge is a broken line. The dead load of the main tower not only produces the stress of the tower body but also produces its bending moment. This affects the entire structural system of the cable-stayed bridge internal force state, so it was necessary to carry out dead load compensation for the main tower.

(3) Bridge pier and support design.

The edge pier and the main pier were welded by steel. The box girder and Pier 4 are connected by bolts. Supports are placed on Piers 3, 5, and 6 with load sensors under each support. A tensile force application device was used to simulate the dead load of the corbel section.

### 3.2. Model construction and installation

A special vibrating wire sensor was used to simulate the stay cable sensor. It was individually calibrated before installation to ensure long-term stability, accuracy, and reliability. We installed the box girder in subsection form to simulate the construction process as accurately as possible. According to the real-world construction requirements, Pier 5 was set as a temporary pier and a load sensor was installed to measure the counter force of the temporary support under the action of the construction load.



Fig. 3. Model test

### **3.3. Cable force test system**

The stay cable and box girder were installed before being gradually compensated for dead load in the actual construction process of the original bridge. The stay cable was tensioned and the cable was adjusted as necessary. The model test system includes a support reaction force test system, dead load test system, stress test system, displacement test system, and cable force test system.

A calibrated strain tester and load sensor were installed at each fulcrum to form a supporting reaction force testing system. The dead load test was directly carried out with a calibrated platform scale. The stress test system is composed of strain gauges and resistance strain gauges. In the experiment, the electrical measurement method was used to test the stress distribution of the live load and constant load structure. The displacement test was carried out with a spirit level, dial indicator, and theodolite. The cable force test system consists of a calibrated special frequency tester and a steel string load cell.

## **4. Optimum Dead Load Cable Force Analysis of Cable-stayed Bridge**

### **4.1. Static Balance Characteristics of Prestressed Concrete Polygonal Line Tower Under Dead Load**

#### **4.1.1. Overall balance characteristics of main girder, main tower**

In prestressed concrete polygonal-line tower cable-stayed bridges, in order to offset the overturning moment caused by the tilt of the main tower itself and to ensure that the main tower is in the proper state of stress, side and mid-span main beams are generated by stay cables on the main tower. The anti-overturning moment must be balanced with the gravity moment of the tower body. Only the symmetrical position of the stay cables on either side of the main tower were given different cable forces in this study, as this balances the force across the polygonal-line tower [20–22].

The following assumptions were made to simplify the calculation process.

- (1) The vertical component of the dead cable force of a single stay cable is equal to the dead weight of the beam. The sum of the vertical components of all cables is equal to the dead weight of the main beam of the cable section.
- (2) The influence of the weight of the main girder of the full bridge without the cable section on the balance of the tower girder structure is ignored.

The overall balance diagram of the polygonal-line tower cable-stayed bridge was obtained in accordance with these assumptions.

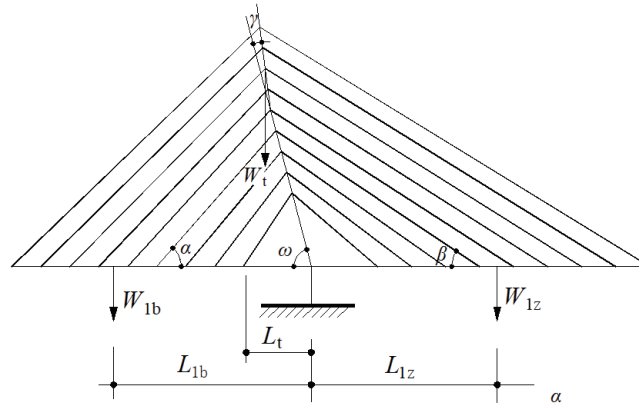


Fig. 4. Global balanced diagram of cable-stayed bridge with polygonal-line tower

In Figure 4,  $W_t$  is the weight of the bridge tower,  $L_t$  is the distance from the center of gravity of the bridge tower to the consolidation point of the beam tower,  $W_{lz}$  is the weight of the main girder in the cable area of the main span, and  $L_{lz}$  is the center of gravity of the main girder in the main span cable area from the consolidation point of the tower distance.  $W_{lb}$  is the weight of the main girder in the side span cable area;  $L_{lb}$  is the distance between the center of gravity of the main girder in the side span cable area and the consolidation point of the beam tower.

According to Figure 4 and the above assumptions, the overturning moment of the main girder of the side span cable section to the beam tower consolidation point, the overturning moment of the bridge tower's weight, and the resistance moment of the main beam of the span cable section to the beam tower consolidation point can be obtained as follows:

$$(4.1) \quad M_{lb} = W_{lb} L_{lb}$$

$$(4.2) \quad M_t = W_t L_t$$

$$(4.3) \quad M_{lz} = W_{lz} L_{lz}$$

The dead load bending moment of the main tower root can be obtained accordingly:

$$(4.4) \quad M = M_t + M_{lb} - M_{lz} = W_t L_t + W_{lb} L_{lb} - W_{lz} L_{lz}$$

To ensure that the root of the polygonal-line tower is in a state of axial compression under constant load, the dead load bending moment at the root of the polygonal-line tower should satisfy  $M = 0$ . At this point, the dead load on the side of the cable-stayed bridge, the mid-span main girder, and the dead weight of the polygonal-line tower are completely balanced. In this state, the polygonal-line tower's root only bears the bending moment caused by the live load and the additional load. The overall balance relationship of the bridge structure can be satisfied only by adjusting the size of the side and mid-span main girder section and the spacing of the cable stays.

#### 4.1.2 Local balance characteristics of main girder and main tower

At the same section, the sum of the moment generated by the tower column's weight and the moment generated by the side span stayed cable force was taken, then the moment generated by the corresponding stayed cable force on the main span was subtracted from this value as the moment of force of that section. The section's moment value is not necessarily zero under the overall equilibrium state of the broken line tower [23–25]. To ensure that each section of the polyline tower meets the force requirements and is in a good state of force, the overall balance of the polyline tower and local force condition of the polyline tower must be firmly established.

A corresponding beam section and tower section were taken arbitrarily from the tower column area under the polygonal-line tower alongside a pair of corresponding stay cables to analyze the local balance relationship, as shown in Figure 5.

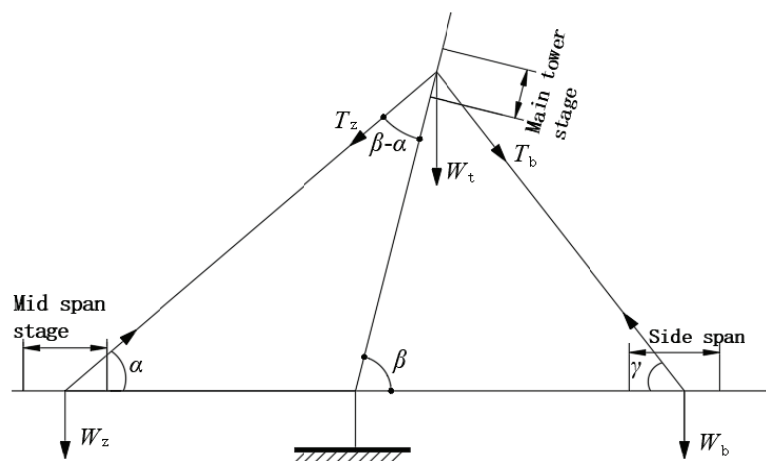


Fig. 5 Local balance diagram of lower tower

It is assumed here that the main span cable force is  $T_z$ , the side span cable force is  $T_b$ , the tower body weight is  $W_t$ , the central span main beam section weight is  $W_z$ , and the side span main beam section weight is  $W_b$ . Under the assumptions under the overall equilibrium state, the cable force's



vertical component value under the dead load state is equal to the load of the main beam section. If the cable force and the component force generated by the tower body weight perpendicular to the tower body are balanced, the resultant horizontal component force is zero. At this point, the broken line tower does not bear the overturning moment; the combined force of the cable force and tower weight falls along the downward direction of the axis of the tower column and the lower tower column is in a state of axial compression.

The partial balance relationship of the polygonal-line tower cable-stayed bridge can be modeled by the following formulas. The cable force of the stay cable corresponds to the load of the main beam section has the following one-to-one relationship:

$$(4.5) \quad W_z = T_z \sin \alpha, \quad T_z = W_z / \sin \alpha$$

$$(4.6) \quad W_b = T_b \sin \gamma, \quad T_b = W_b / \sin \gamma$$

The resultant force is zero perpendicular to the direction of the tower body:

$$(4.7) \quad T_z \sin(\beta - \alpha) = W_t \cos \beta + T_b \cos(\beta + \alpha - 90)$$

According to Formulas (4.2)–(4.6):

$$(4.8) \quad W_t = \frac{T_z \sin(\beta - \alpha) - T_b \cos(\beta + \gamma - 90)}{\cos \beta}$$

and further:

$$(4.9) \quad W_t = \frac{W_z \sin(\beta - \alpha) \sin \gamma - W_b \cos(\beta + \gamma - 90) \sin \alpha}{\sin \alpha \sin \gamma \cos \beta}$$

This is the dead load local balance formula of the beam and tower of the polygonal-line tower cable-stayed bridge's lower tower column. The dead load local balance formula of the beams and towers of the upper tower column can be obtained similarly according to the upper tower column section force (Figure 6).

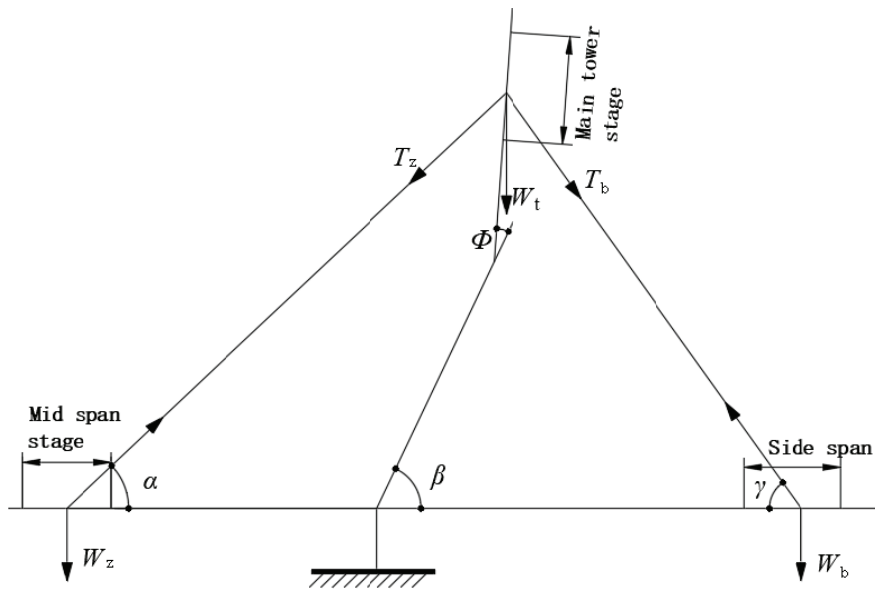


Fig. 6 Local balance diagram of upper tower

$$(4.10) \quad W_t = \frac{W_z \sin(\beta + \phi - \alpha) \sin \gamma - W_b \cos(\beta + \phi + \gamma - 90) \sin \alpha}{\sin \alpha \sin \gamma \cos(\beta + \phi)}$$

The above partial balance formula confirms that the cable arrangement of the bridge and the inclination of the central tower are important geometric parameters in a polygonal-line tower cable-stayed bridge design. The main girder can be adjusted in the design process as the weight distribution of the side and middle span can be used to balance the main tower.

## 4.2 Cable force determination

The overall balance and local balance formulas of the prestressed concrete polygonal-line tower cable-stayed bridge can be used to preliminarily design its main structural dimensions as a basic condition for further cable force optimization. This is a step-wise process.

(1) The prestressed concrete polygonal-line tower cable-stayed bridge's dead load state is initially determined via the minimum bending energy method. According to the structure size described above, without considering the main girder's prestress design, the minimum bending energy method was used here to analyze and optimize the bridge according to the determined structure size.

(2) The prestressed concrete polygonal-line tower cable-stayed bridge is calculated by the dummy load method. According to the preliminarily determined reasonable bridge state, the bridge's live load calculation is carried out and converted into the virtual load (dummy load) [26–27]. The dummy load can be taken as half of the live design load equivalent to a uniform load; the whole

bridge is covered. The internal force of each control section of the central tower and main beam are necessary to adjust the bending moment. Here, a virtual load (dummy load) was applied to produce the expected value of the internal force on the control section so that the bending moment value of each control section in the most unfavorable load combination fell within the allowable range [28].

(3) Calculate the least favorable stress envelope diagram of the main beam and pylon. In this step, the false load is canceled using the completed state of the prestressed concrete polygonal-line tower cable-stayed bridge obtained in the previous step. and the internal force of the bridge generated by other load factors (eg, concrete shrinkage and creep, motor vehicle loads) can then be considered to determine the worst-case stress envelope diagram of the winning beam and pylon.

(4) Design the main beam prestress characteristics. According to the internal force balance method, the central girder stress envelope diagram (Formula (4.2)) is used to establish the pre-stress design of the main girder. The least favorable stress envelope diagram of the main girder can then be calculated. The magnitude and eccentricity of the pre-energizing force are adjusted to make the primary beam stress meet the requirements [2].

(5) Simulate the actual construction process to carry out forward installation calculation of the bridge. The prestressed design of the main girder calculated in the previous step was used here to simulate the actual construction process, then the bridge was simulated again to determine its final state. The cable force is the reasonable dead load cable force of the prestressed concrete polygonal-line tower cable-stayed bridge.

## 5. Dead load cable force analysis

It is convenient to analyze the cable force distribution of the prestressed concrete polygonal-line tower cable-stayed bridge, calculate the cable force and design cable force according to Formula (3.1), and convert the cable force distribution into a cable force column as shown in Figures 7–8. The measured cable force, calculated cable force, and designed cable force are similar, except for individual cables. Significant deviations in cable force can be found the first three pairs of short cables. The short cables are rigid, so small construction errors (e.g., tension errors, structural rigidity deviations) create substantial deviations in cable force. The short cable's strength should be greater than that of the long cable in the design.

Additionally, because the dead load of the model test is compensated by the concentrated load, the tension cable force was directly used after conversion according to the design cable force of the real bridge. This caused a certain deviation between the calculated cable force of the model and the

actual value. The average deviation between the cable force calculated by the model and the designed cable force is 2% for Pier 4 and 3% for Pier 5. The average deviation between the measured cable force and the bridge's designed cable force is 3% on Pier 4 and 5% on Pier 5.

Table 1. Pier 4 cable force histograms

(a) Comparison of test and calculation bridge cable force values, Pier 4

Cable	C15	C14	C13	C12	C11	C10	C9	C8
Calculated bridge tension force	8540	10810	11100	11260	11490	11250	10660	10860
Converted value	5.34	6.76	6.94	7.04	7.18	7.03	6.66	6.79
Test tension force	5.47	7.05	7.01	7.06	6.99	7.29	6.75	6.87
Cable	C7	C6	C5	C4	C3	C2	C1	C1'
Calculated bridge tension force	10050	9630	9580	10140	9870	12220	11260	9680
Converted value	6.28	6.02	5.99	6.34	6.17	7.64	7.04	6.05
Test tension force	6.18	5.86	5.76	6.28	5.91	7.45	5.74	5.81
Cable	C2'	C3'	C4'	C5'	C6'	C7'	C8'	C9'
Calculated bridge tension force	9970	6060	6450	6370	6400	6190	6690	6510
Converted value	6.23	3.79	4.03	3.98	4.00	3.87	4.18	4.07
Test tension force	5.86	3.66	4.1	4.15	4.12	3.99	4.4	4.15
Cable	C10'	C11'	C12'	C13'	C14'	C15'	–	–
Calculated bridge tension force	7200	7180	10940	11180	12210	11780	–	–
Converted value	4.5	4.49	6.84	6.99	7.63	7.36	–	–
Test tension force	4.53	4.42	6.93	7.19	8.05	7.63	–	–

(b) Comparison between test and design cable force values, Pier 4

Cable	C15	C14	C13	C12	C11	C10	C9	C8
Design bridge tension force	8330	11700	11900	12000	12000	11700	11400	11500
Converted value	5.34	6.76	6.94	7.04	7.18	7.03	6.66	6.79
Test tension force	5.47	7.05	7.01	7.06	6.99	7.29	6.75	6.87
Cable	C7	C6	C5	C4	C3	C2	C1	C1'
Design bridge tension force	10600	10200	10100	8780	8430	11800	10500	9970
Converted value	6.28	6.02	5.99	6.34	6.17	7.64	7.04	6.05
Test tension force	6.18	5.86	5.76	6.28	5.91	7.45	5.74	5.81
Cable	C2'	C3'	C4'	C5'	C6'	C7'	C8'	C9'
Design bridge tension force	10400	5940	6320	6390	6560	6430	7060	6970
Converted value	6.23	3.79	4.03	3.98	4.00	3.87	4.18	4.07
Test tension force	5.86	3.66	4.1	4.15	4.12	3.99	4.4	4.15
Cable	C10'	C11'	C12'	C13'	C14'	C15'	–	–
Design bridge tension force	7540	7600	11700	12000	13700	12500	–	–
Converted value	4.5	4.49	6.84	6.99	7.63	7.36	–	–
Test tension force	4.53	4.42	6.93	7.19	8.05	7.63	–	–

The two main towers' boundary conditions are different under the dead load, but the cable force of the stay cables is mainly comprised of the dead load. The two main towers' total cable force should be in accordance to balance the bridge and ensure the minimum bending energy across the structure with the broken line tower. The bridge's inclination angle gradually decreases due to the angle of the tower column, and the upper tower column is nearly vertical. In order to satisfy the local balance of the polygonal-line tower cable-stayed bridge, the cable force is distributed from large to small, then from small to large, from near to far away from the central tower.

The results also show that the polygonal-line tower is inclined to the side span. To balance the central tower's weight, the mid-span cable force should be greater than the side span cable force. The two main towers have different boundary conditions, so to ensure their internal forces are in accordance at the corresponding positions, the internal force and deformation of the beam should be close while the corresponding cable forces at the two main tower positions are different.

## 6. Conclusion

This paper proposed a novel method for determining the reasonable design and optimal dead load cable force in a cable-stayed bridge. The mechanical characteristics of the overall balance and local balance of a prestressed concrete polygonal-line tower cable-stayed bridge were determined, then the proper reference size of the bridge design was determined. The Fumin Bridge in Shenyang was taken as a case study to optimize the cable force of an actual prestressed concrete polygonal-line tower cable-stayed bridge. The main conclusions can be summarized as follows.

- (1) The cable arrangement and central tower inclination are important geometric parameters for the design of the polygonal-line tower cable-stayed bridge. Adjusting the weight distribution of the primary beam side and mid-span can balance the central tower's weight in the design stage.
- (2) The cable-stayed bridge's inclination angle gradually decreases due to the angle of the tower column; the upper tower column is nearly vertical. To satisfy the local balance of the bridge, the cable force is distributed from large to small, and then from small to large, from near to far away from the central tower.

The polygonal-line tower is inclined to the side span, so to balance the central tower's weight, the mid-span cable force should be greater than the side span cable force. The two main towers have different boundary conditions, so to ensure that their internal forces are uniform and fall into the proper positions, the internal force and deformation of the beam should be close while the corresponding cable forces at the main tower positions should be different.

## References

- [1] E. Atashpaz-Gargari, C. Lucas. „Imperialist competitive algorithm: an algorithm for optimization inspired by imperialistic competition”. [J] Proceedings of 2007 IEEE Congress on Evolutionary Computation. Singapore: IEEE, 2007: pp. 4661–4667.
- [2] A. Kaveh, S. Talatahari. “Optimum design of skeletal structures using imperialist competitive algorithm”. [J] Computers and Structures, 2010, 88: pp. 1220–1229.
- [3] M. M. Hassana, A. O. Nassef, E. Damatty. “Determination of optimum post-tensioning cable forces of cable-stayed bridges”. [J] Engineering Structures, 2012(1): pp. 248–259.
- [4] Z. J. Chen, Y. Liu, L. F. Yang. “Optimization of Stay Cable Tension of Completed Bridge of Single-Pylon Cable-Stayed Bridge Based on Particle Swarm Optimization Algorithm”. [J] Bridge Construction, 2016 46(3): pp. 40–44.
- [5] S. Q. Qin, Z. Y. Gao. „Developments and Prospects of Long-Span High-Speed Railway Bridge Technologies in China”. [J] Engineering, 2017, 3(6): pp. 787–794.
- [6] J. L. Wang, L. He. “A Prestressing Tendon Element Geoenvironmental Engineering”, 2013, 139(8): pp. 1262–1274.
- [7] T. Carey, B. Mason, A. R. Barbosa, et al. “Modeling Framework for Soil-bridge System Response during Sequential Earthquake and Tsunami Loading”. [C] Tenth US National Conference on Earthquake Engineering, Anchorage [s.n.], 2014.
- [8] H. Tao, X. F. Shen. “Strongly subfeasible sequential quadratic programming method of cable tension optimization for cable-stayed bridges”. [J] Chinese Journal of Theoretical and Applied Mechanics, 2006, 38(3): pp. 381–384. (in Chinese)

- [9] X. H. Zhou, P. Dai, D. Jin. "Optimization analysis of cable tensions of dead load state for cable-stayed bridge with steel box girder" [J] *Journal of Architecture and Civil Engineering*, 2007, 24(2): pp. 19–23. (in Chinese)
- [10] A. Baldomir, S. Hernandez, F. Nieto, et al. "Cable optimization of along span cable stayed bridge in La Coruña (Spain)". [J]. *Advances in Engineering Software*, 2010,41: pp. 931–938.
- [11] A. M. B. Martins, L. M. C. Simoes, J. H. J. O. Negro. "Optimization of cable forces on concrete cable-stayed bridges including geometrical nonlinearities". [J] *Computers and Structures*, 2015, 155: pp. 18–27.
- [12] M. M. Hassan, A. A. El Damatty, A. O. Nassef. "Database for the optimum design of semi-fan composite cable-stayed bridges based on genetic algorithms". [J] *Structure and Infrastructure Engineering*, 2014, 11(8): pp. 1054–1068.
- [13] X. Wu, R. C. Xiao. "Optimization of cable force for cable-stayed bridges with mixed stiffening girders based on genetic algorithm". [J] *Journal of Jiangsu University (Natural Science Edition)*, 2014, 35(6): 2016, 12(2): pp. 208–222.
- [14] Y. C. Sung, C. Y. Wang, E. H. Teo. "Application of particle swarm optimisation to construction planning of cable-stayed bridges by the cantilever erection method". [J] *Structure and Infrastructure Engineering*, 2016, 12(2): pp. 208–222.
- [15] B. S. Smith. "The Single a Palne Cable-stayed Girder Bridge: a Method of Analysis Suitable for Computer Use". [J] *Civil engineering*, 1967,37(5): pp.183–194.
- [16] Y. Xi; J. S. Kuang. "Ultimate Load Capacity of Cable-stayed Bridge". *Journal of Bridge Engineering* [J]. 1999, 4(1): pp. 14–22.
- [17] C. Honigmann, D. Billington. "Conceptual Design for the Sunniberg Bridge" [J] *Journal of bridge engineering*, 2003, 8(3): pp. 122–130.
- [18] R. Karoumi. "Some modelling aspects in the nonlinear finite element analysis of cable supported bridges". [J] *Computers & Structures*, 1999, 71(4): pp. 397–412.
- [19] Q. S. Chen, W. L. Huang, M G Yang, "Analysis of shear lag effect in construction stage of wide box girder extradosed cable-stayed bridge with large flanges", *Journal of Railway Science and Engineering*, vol. 15, no. 12, pp. 3158–3164, 2018.
- [20] X. Guo, Y. K. Wu, Y. Guo. "Time-dependent Seismic Fragility Analysis of Bridge Systems under Scour Hazard and Earthquake Loads". [J] *Engineering Structures*, 2016, 121: pp. 52–60.
- [21] M. M. Chiaramonte, P. Arduino, D. E. Lehman, et al. "Seismic Analyses of Conventional and Improved Marginal Wharves". [J] *Earthquake Engineering & Structural Dynamics*, 2013, 42(10): pp. 1435–1450.
- [22] A. E. Haiderali, G. Madabhushi. "Evaluation of Curve Fitting Techniques in Deriving P-Y Curves for Laterally Loaded Piles". [J] *Geotechnical and Geological Engineering*, 2016, 34(5): pp. 1453–1473.
- [23] M. H. Faber, S. Englund, R. Rackwitz. "Aspects of parallel wire cable reliability". [J] *Structural Safety*, 2003, 25(2): pp. 201–225.
- [24] C. M. Lan, N. N. Bai, H. T. Yang, et al. "Weibull modeling of the fatigue life for steel rebar considering corrosion effects". [J] *International Journal of Fatigue*, 2018, 111: pp. 134–143.
- [25] C. M. Lan, Y. Xu, C. P. Liu, et al. "Fatigue life prediction for parallel-wire stay cables considering corrosion effects". [J] *International Journal of Fatigue*, 2018, 114: pp. 81–91.
- [26] M Bruneau. "Evaluation of system-reliability methods for cable-stayed bridge design". [J] *Journal of Structural Engineering*, 1992, 118(4): pp. 1106–1120.
- [27] Y. Liu, N. W. Lu, X. F. Yin, et al. "An adaptive support vector regression method for structural system reliability assessment and its application to a cable-stayed bridge". [J] *Proceedings of the Institution of Mechanical Engineers, Part O: Journal of Risk and Reliability*, 2016, 230(2): pp. 204–219.
- [28] V. Lute, A. Upadhyay, K. K. Singh. "Computationally efficient analysis of cable-stayed bridge for GA-based optimization". [J] *Engineering Applications of Artificial Intelligence*, 2009, 22: pp. 750–758.

Received: 22.01.2021, Revised: 12.04.2021